arXiv:1406.6727v1 [astro-ph.SR] 25 Jun 2014

Asociación Argentina de Astronomía
BAAA, Vol. 56, 2013
A.C. Rovero, P.B. Tissera, L.J. Pellizza & M. Lares, eds.

PRESENTACION INVITADA

Stellar Variability in the VVV Survey: An Update

M. Catelan[1,2], I. Dékány[2,1], M. Hempel[1,2] & D. Minniti[1,2]

(1) Pontificia Universidad Católica de Chile, Facultad de Física, Instituto de Astrofísica, Santiago, Chile
(2) Millennium Institute of Astrophysics, Santiago, Chile

Abstract. The *Vista Variables in the Vía Láctea* (VVV) ESO Public Survey consists in a near-infrared time-series survey of the Galactic bulge and inner disk, covering 562 square degrees of the sky, over a total timespan of more than 5 years. In this paper, we provide an updated account of the current status of the survey, especially in the context of stellar variability studies. In this sense, we give a first description of our efforts towards the construction of the *VVV Variable Star Catalog* (VVV-VSC).

Resumen. El Relevamiento Público ESO titulado *Variables Vista en la Vía Láctea* (VVV) consiste en un relevamiento con resolución temporal del bulbo y disco interno Galácticos en el infrarrojo cercano, cubriendo 562 grados cuadrados del cielo, en un intervalo de tiempo de más de 5 años. En este artículo, entregamos una descripción actualizada del estado actual del relevamiento, especialmente en el ámbito de los estudios de variabilidad estelar. En ese sentido, describimos, por primera vez, nuestros esfuerzos para la construcción del *Catálogo de Estrellas Variables* del VVV (VVV-VSC).

1. Overview

The Vista Variables in the Vía Láctea (VVV) ESO Public Survey (Minniti et al. 2010; Catelan et al. 2011; Saito et al. 2012; Hempel et al. 2014) is a time-series, near-infrared (IR) survey of the Galactic bulge and an adjacent portion of the inner disk, covering 562 square degrees of the sky. The survey, which is based on images taken with the VIRCAM camera mounted on the VISTA telescope, located in Cerro Paranal, northern Chile, has provided multi-color photometry in 5 broadband filters (Z, Y, J, H, and K_s), but its main goal is to provide a homogeneous database for variability studies of the observed regions, particularly in the K_s band.

An extensive overview of recent work on stellar variability that has been carried out in the framework of the VVV Survey has been presented by Catelan et al. (2013). Here we provide a brief update on the status of the survey, particularly in regard to our ongoing work on stellar variability.

2. Status of the Survey

Figure 1 shows the complete area covered by VVV, with the different "tiles" (which constitute individually observed fields) indicated as red squares. Each tile covers 1.501 deg^2 in the sky, and the survey encompasses 348 tiles in total. For each VVV tile, Figure 1 also shows its ID number (*upper label*) and the number of epochs in K_s that have been obtained, as of this writing (*bottom label*). As far as the cadence, Figure 2 shows the delay (i.e., time interval) between two successive epochs in the VVV K_s-band data, color-coded according to the scale on the right of each plot. By the end of the survey, the bulge region will contain between 60 and 100 epochs for each tile, whereas the disk tiles will have ≈ 60 epochs each.

Figure 3 shows some examples of VVV light curves for bulge RR Lyrae stars. These stars had been previously identified by the OGLE-III survey (Soszyński et al. 2011), and so their pulsation periods are accurately known. The VVV light curves of known RR Lyrae with very accurately known periods will enable us to systematically investigate, with unprecedented detail, the near-infrared light-curve properties of these stars: note, for instance, how the three RR Lyrae stars shown in Figure 3 have different light-curve morphologies, in spite of their very similar periods. Such detailed studies of light-curve morphology will be important for constraining pulsation models (e.g., Bono et al. 2000).

Using such well-defined K_s-band light curves, we will also study possible relationships between near-infrared light-curve parameters and the metallicity (in addition to stellar physical parameters), as has been done many times previously in the optical for different types of variables, most notably Cepheids and RR Lyrae stars (e.g., Simon & Lee 1981; Simon & Teays 1982; Jurcsik & Kovács 1996; Kovács & Walker 2001; Morgan et al. 2007; Nemec et al. 2013). In turn, this might prove very useful for studying the metallicity distributions/gradients of the stellar populations that these stars trace – i.e., in the bulge and the thick disk, in the case of RR Lyrae stars (e.g., Layden 1995).

In like vein, by combining RR Lyrae light curves from visual databases and VVV light curves, we are in a position to simultaneously derive extinction and distance *to each individual star*. This can be achieved by applying the RR Lyrae period-luminosity calibrations in the visual and near-infrared bands, such as provided by Catelan et al. (2004) in I, J, H, and K. A first such application has recently been described by Dékány et al. (2013), where bulge RR Lyrae stars in common between the OGLE and VVV surveys were used, together with the Catelan et al. period-luminosity relations, to infer an RR Lyrae-based distance to the Galactic center, estimated at $R_0 = 8{,}33 \pm 0{,}05 \pm 0{,}14$ kpc, where the indicated error bars correspond to the estimated statistical and systematic uncertainties, respectively. This is in remarkable agreement with the dynamical value derived by Gillessen et al. (2009), who have obtained $R_0 = 8{,}35 \pm 0{,}35$ kpc by studying the orbits of stars around the Galaxy's central black hole.

The very complete VVV light curves for many different types of variable stars will also be useful as templates – and indeed, many such reliably classified light curves with complete phase coverage have already been incorporated into the so-called *VVV Templates Database* (Angeloni et al. 2014),[1] whose main

[1] `http://vvvtemplates.org/`

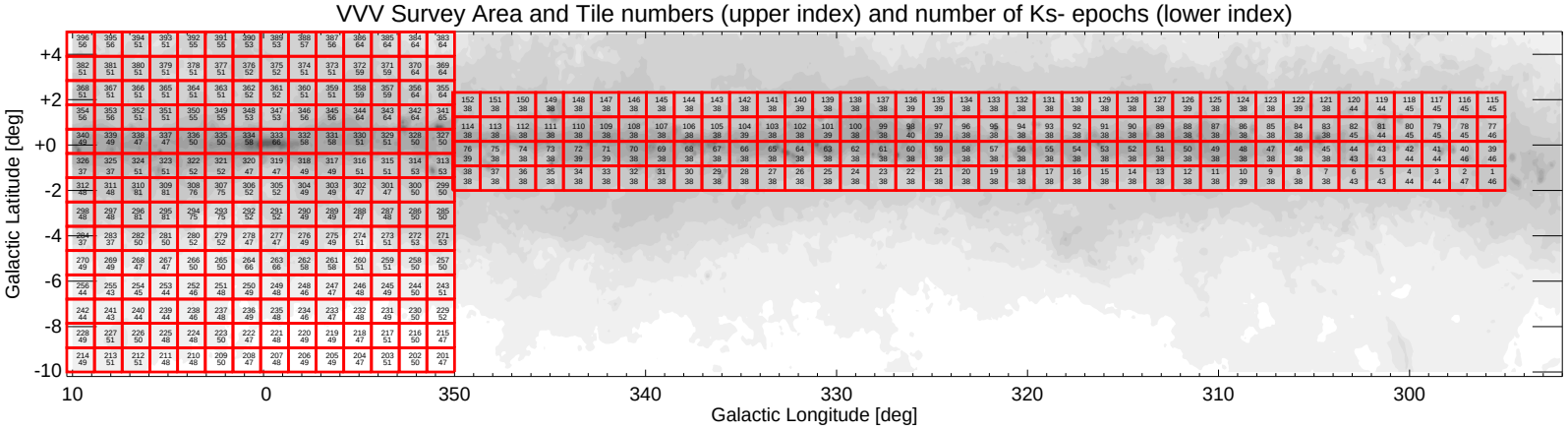

Figura 1. VVV Survey area, superimposed on a gray-scale image that represents the Galactic dust extinction maps by Schlegel et al. (1998). Each of the 348 tiles of the survey is represented by a red rectangle, and is identified by its ID number (*upper label* within each tile). Each such tile, which covers a ≈ 1.5 square degree field, has already been observed at least once in each of the Z, Y, J, H, and K_s filters. The actual number of epochs in the K_s-band as of this writing (May 16, 2014) is shown underneath each tile's ID number.

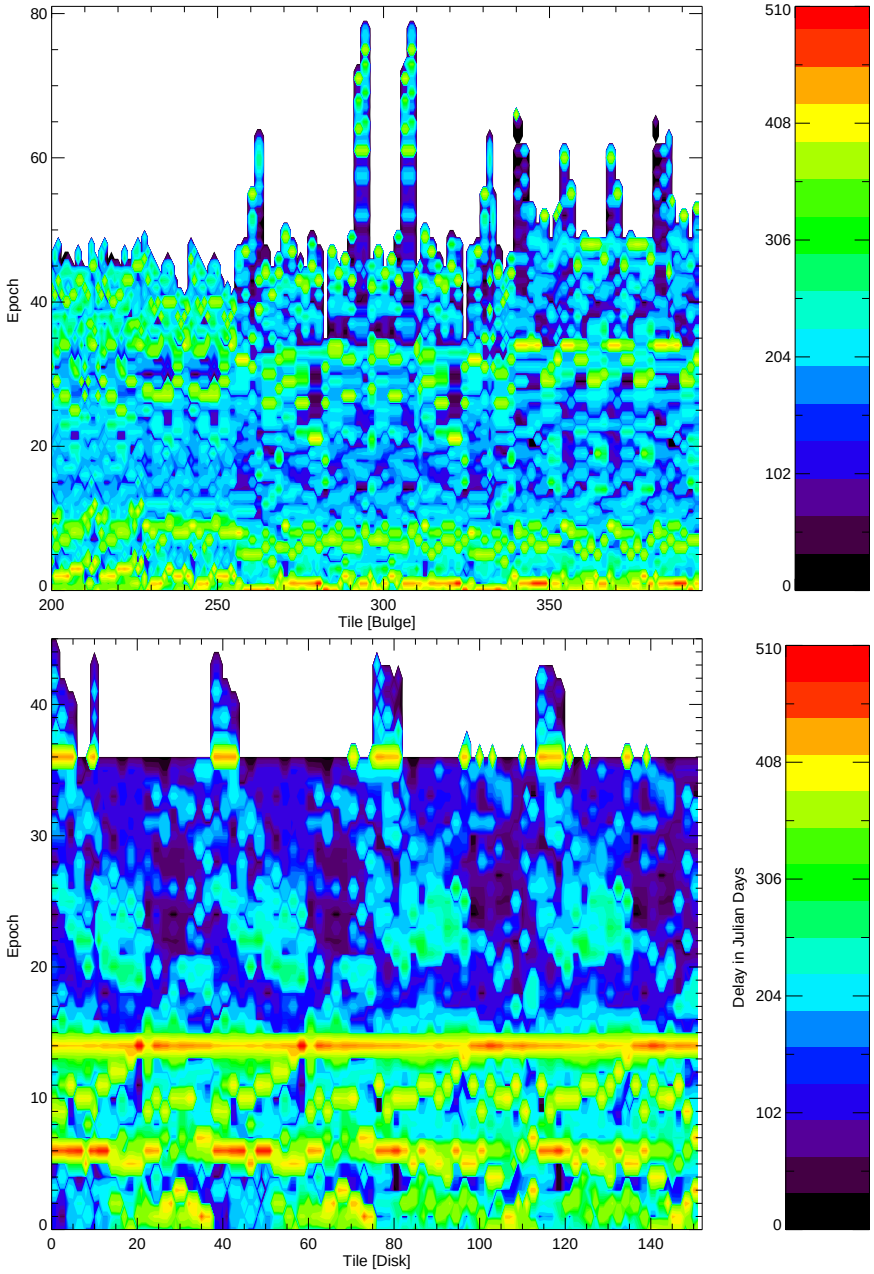

Figura 2. Time delay (in Julian Days) between two consecutive epochs of K_s-band observations for the bulge (*top*) and disk (*bottom*) tiles, based on all VVV time-series data obtained as of this writing (May 16, 2014). The 8 tiles with the largest number of observed epochs (ID numbers: 293, 294, 295, 296, 307, 308, 309, 310; see also Fig. 1) are bulge tiles situated in Baade's Window, with a much reduced dust extinction and for which independent observations are available in the optical bands from the OGLE survey (Udalski et al. 1992).

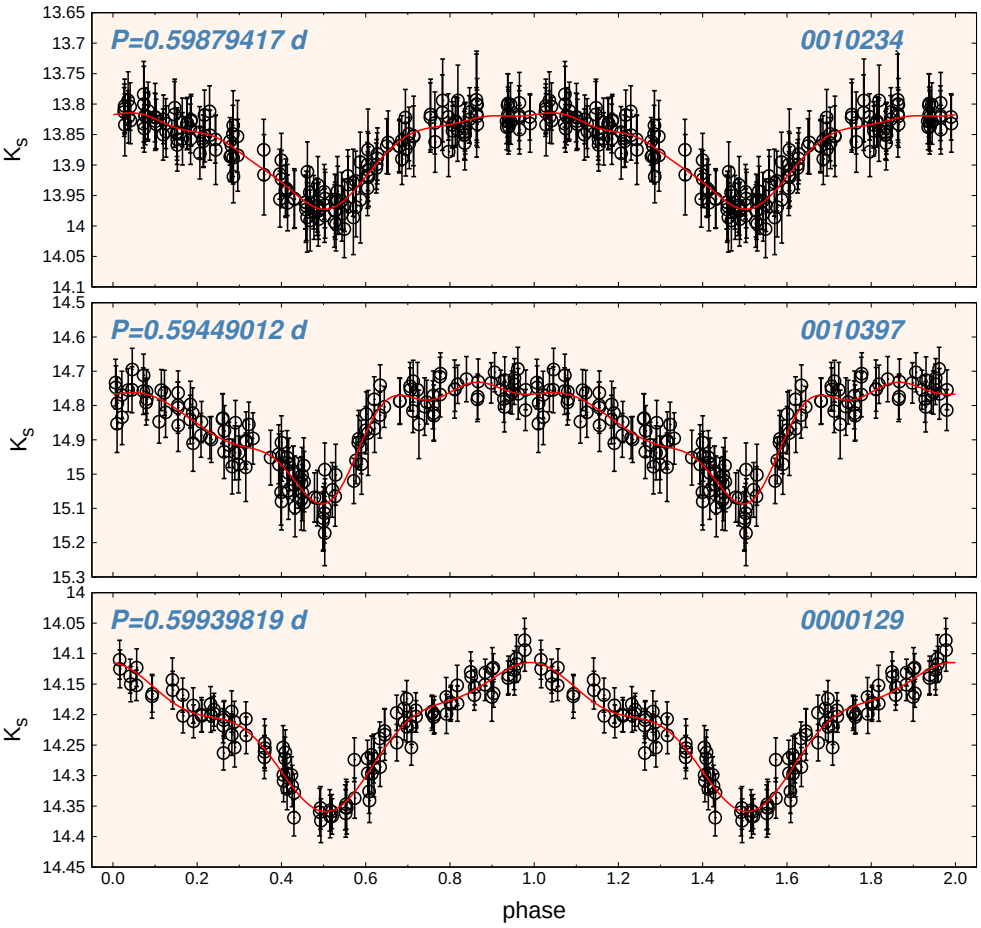

Figura 3. These panels show the K_s-band phase diagrams of 3 bulge ab-type (i.e., fundamental-mode) RR Lyrae stars known from the OGLE-III survey (Soszyński et al. 2011; OGLE IDs and periods are shown for each star), illustrating the high quality of the data obtained in the course of the VVV Survey. Note that these three stars have very similar periods, yet quite different light-curve shapes. The *red lines* show the Fourier fits with optimized numbers of terms. The figure includes data obtained up to the end of June 2013.

purpose is to feed the classification algorithms that are currently being devised, in order to perform automated classification of the expected 10^{6-7} variable stars detected in the course of the VVV Survey (Catelan et al. 2011, 2013). It is worth noting, in this regard, that our team has also recently completed a variable star catalog (Ferreira Lopes et al. 2014) using data from the 3.8m United Kingdom Infrared Telescope's (UKIRT) Wide-Field near-IR CAMera (WFCAM; Casali et al. 2007) calibration database. This multi-band database has also yielded high-quality lightcurve templates, which have also been incorporated into the VVV Templates Database (Angeloni et al. 2014).

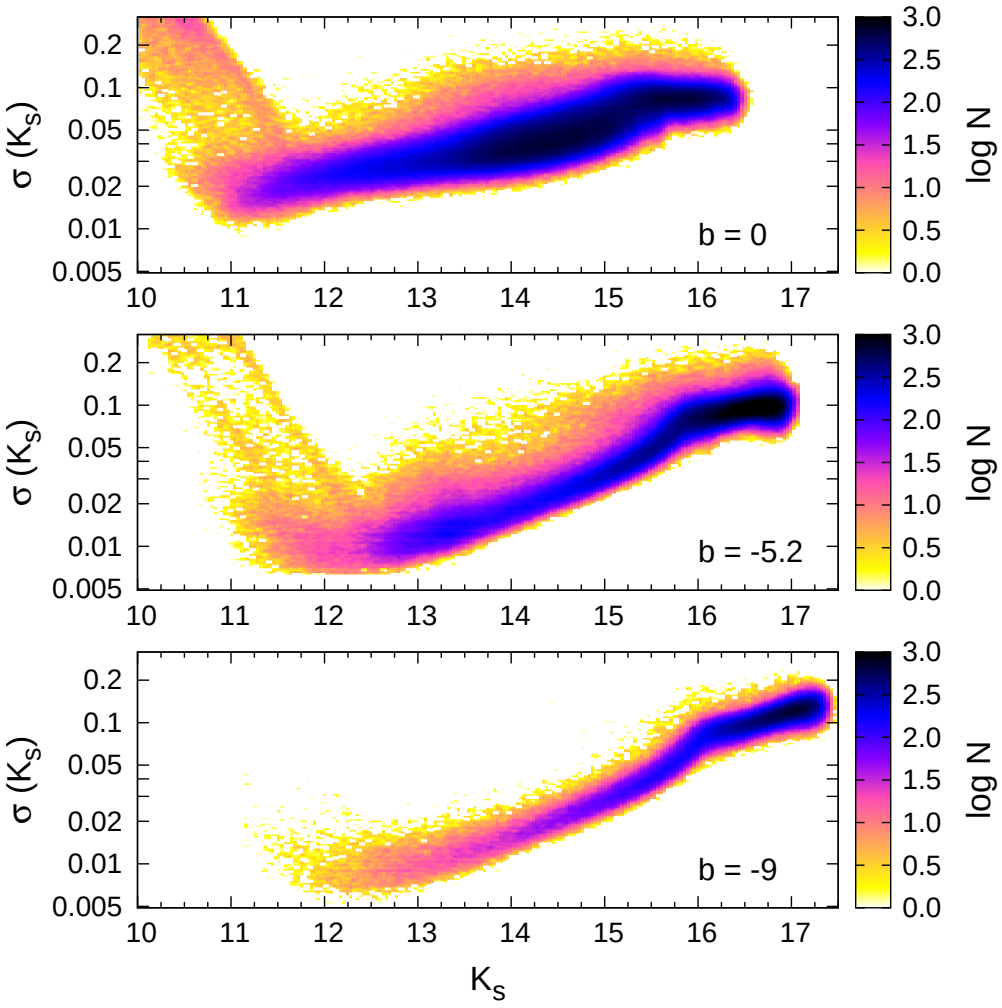

Figura 4. This figure shows the number density distribution of the weighted K_s-band average magnitude vs. the weighted standard deviation of the K_s light curves, for 3 tiles at Galactic longitude $\ell = -2^{\rm o}$ and at different latitudes, namely $b = 0$ (*top*), $-5{,}2^{\rm o}$ (*middle*), and $-9^{\rm o}$ (*bottom*). The plots illustrate the large changes in the noise distribution of the light curves as an effect of increasing source crowding towards the Galactic plane. The deviations from the main locus at magnitudes < 12 mag are due to (temporal) saturation. Note that the color scale, mapped on the right, indicates the logarithm of the number of sources in each bin.

3. VVV-VSC: The VVV Variable Star Catalog

VVV is a public survey, and so one of our main objectives is to provide a variable star catalog (VSC) that will ultimately be useful to the whole astronomical community. Since we last described our work on stellar variability in the framework of the VVV Survey (Catelan et al. 2011, 2013), we have made much progress at building a comprehensive, science-ready relational database of variable VVV

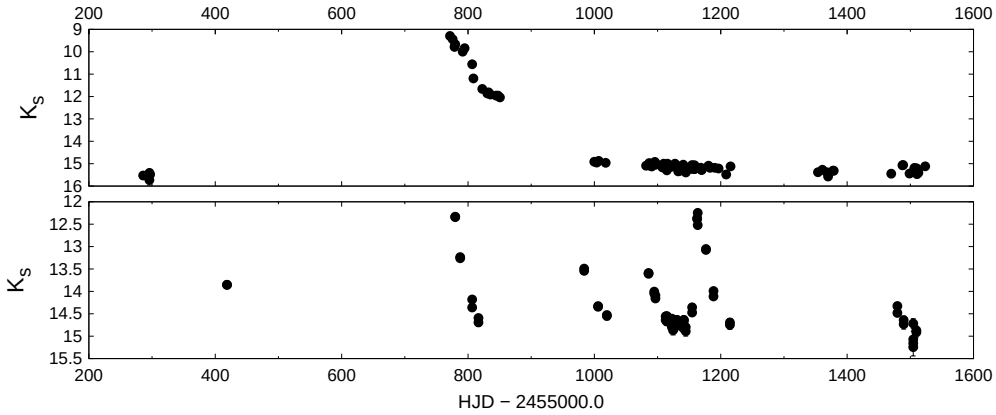

Figura 5. Examples of transient sources in the VVV data. The *upper panel* shows the K_s-band light curve of VVV-WIT-02 (Dekany et al. 2014), which is probably a recurrent nova. The *bottom panel* shows the VVV K_s-band light curve of the candidate young stellar object (YSO) called SSTGLMC G353.4039-00.0664 (Robitaille et al. 2008), which is located in tile b329 (in the bulge plane), previously known from GLIMPSE. The star has a large-amplitude recurring outburst with an approximate period of about 95 days.

point sources. In its current incarnation, the VVV-VSC uses the high-quality aperture photometry provided by the Cambridge Astronomy Survey Unit (CASU; see Catelan et al. 2013, for more details and extensive references). The pipeline first extracts a master source list from the CASU tile catalogs, and then cross-matches those sources with the individual "pawprints" that are used to build each tile (six pawprints per tile; Minniti et al. 2010). Zero-point errors are then added, a threshold rejection procedure applied, aperture optimization carried out (by means of a minimization of the rms scatter), and descriptive statistics computed. Using a number of variability indices (e.g., Welch & Stetson 1993; Stetson 1996; Ferreira Lopes et al. 2014), a list of variable star candidates is then finally obtained. Typically, we have been encountering of order 50,000 candidates per VVV tile.

Current tests indicate that our procedure is highly successful at recovering variable stars in general, and particularly periodic sources with sufficiently high amplitudes in the near-IR. At present, the procedure does not perform well for variable sources such as the following: very fast transients coming from below detection; high-proper motion objects; extremely faint sources; very blue, faint sources; highly crowded sources; and very bright variables (i.e., $\langle K_s \rangle \lesssim 12$ mag), which are commonly saturated in the VVV images. Figure 4 illustrates the mean scatter of the recovered variable star candidates as a function of the mean K_s-band magnitude at three different Galactic latitudes, where the effects of saturation, crowding, and image depth are all apparent.

Naturally, not all variables detected in the VVV data are periodic, and many different examples of variable stars that are not strictly periodic are shown, for instance, in Catelan et al. (2013) and Saito et al. (2013). However, many of the detected variables, such as Cepheids, RR Lyrae, and eclipsing binary stars, *are*

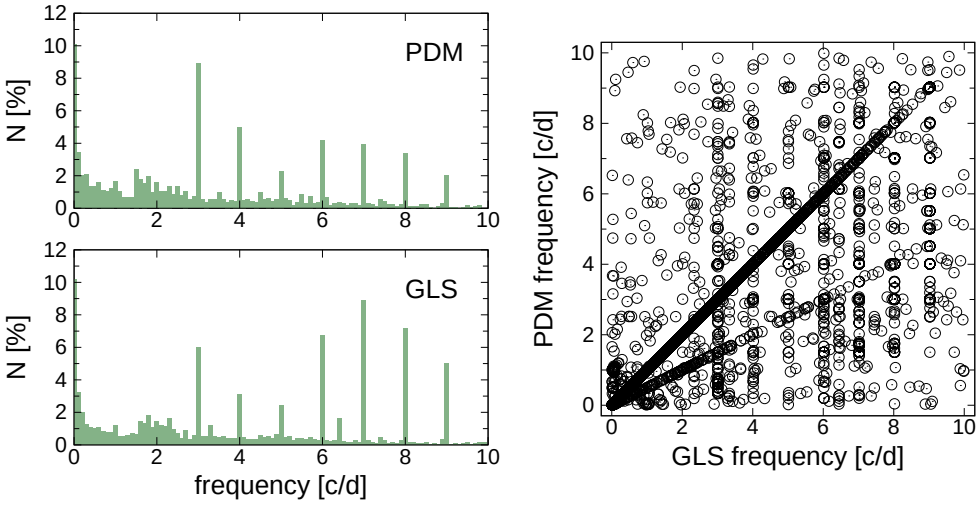

Figura 6. (*left panel*) This plot shows the histograms of the principal frequencies detected by the two methods employed by the VVV variability pipeline, namely PDM (*top*) and GLS (*bottom*), after all the contributions from signals in the $10/T_{\rm tot}$ vicinity of integer c/d frequencies have been removed – where $T_{\rm tot}$ is the total time span covered by the data. The distributions are rather flat, but a small bump due to RR Lyrae stars can be spotted. The peaks at higher frequencies, close to integers and half-integers, are spurious signals, caused mostly by the rotating diffraction spikes around bright stars. The *right panel* shows the consistency between the frequencies detected by the two methods. Most are in agreement, as indicated by the high concentration of points around the 45-degree line overplotted on the data. There is, however, an additional sequence, with GLS periods that are half the PDM periods. This sequence is primarily due to eclipsing binary stars where the GLS algorithm recovers half the true orbital period, due to its diminished sensitivity to the presence of alternating peaks, compared to PDM.

periodic – and thus, once the variable stars are selected following the described procedure, we also carry out a frequency analysis, in order to find periodic and long-term signals, as may be present for each individual star. Figure 5 shows an example of non-periodic transient events detected in our data. To derive the periods, we currently use two different algorithms, namely the generalized Lomb-Scargle periodogram (GLS; Zechmeister & Kürster 2009) and phase-dispersion minimization (PDM; Stellingwerf 1978).

Figure 6 compares the principal frequencies detected by the GLS and PDM methods. Most of the derived periods are in excellent agreement, as indicated by the large concentration of points around the 45-degree line that is overplotted in this diagram. However, a secondary sequence is also present, representing favored GLS periods which are half as long as the corresponding PDM periods. Close inspection of the light curves of stars falling along this sequence reveals that it is mostly caused by eclipsing binary stars for which GLS incorrectly favors a period that is half as long as the true orbital period. This is caused by GLS's reduced sensitivity to the presence of alternating peaks in the time series, compared to

PDM. Note also the presence of a large number of spurious detections at integer and half-integer periods. Most of these variable star candidates are actually *not* intrinsically variable, but represent instead stars in the vicinity of bright sources, whose spurious, periodic "variability signal" is actually produced by the rotating diffraction spike pattern that is seen around these very bright stars.

By the end of the survey, once the VVV-VSC catalog is completed, we will be in a position to provide a relational database containing variability information for up to several million point sources. Our variability tables will include detailed information on the degree of variability, including for instance mean, median, minimum and maximum magnitudes, standard deviations, rms scatter, skewness, kurtosis, etc.; frequency analysis tables, including information on the power spectra and the periods derived therefrom; and queryable light curves and plots, enabling the display and retrieval of data (both raw and processed) in all 5 bandpasses used in the survey (Sect. 1.).

4. Conclusions

The VVV ESO Public Survey provides a treasure trove of scientific data that can be exploited in numerous different scientific contexts. In terms of stellar variability, the project will provide up to several million calibrated K_s-band light curves for genuinely variable sources, including pulsating stars, eclipsing systems, rotating variables, cataclysmic stars, microlenses, planetary transits, and even transient events of unknown nature. In this paper, we have provided a brief overview of the current status of the survey, as far as detection, cataloging, and classification of variable point sources is concerned.

VVV is a public survey, and so the data will quickly be made available to the entire astronomical community as we move along, thus opening the door to many additional applications and synergies with other ongoing and future projects that target the same fields as those covered by VVV. In this sense, in this paper we have also described our current efforts at creating the VVV Variable Star Catalog (VVV-VSC) – a fully queryable relational database that will allow users to quickly and efficiently retrieve variability and frequency analysis tables for the sources detected, multi-band color information, and – last but not least – the light curves themselves.

Acknowledgements. The VVV Survey is supported by the European Southern Observatory, the Basal Center for Astrophysics and Associated Technologies (PFB-06), and the Chilean Ministry for the Economy, Development, and Tourism's Programa Iniciativa Científica Milenio through grant P07-021-F, awarded to The Milky Way Millennium Nucleus. M.C. gratefully acknowledges the support provided by Fondecyt through grant #1141141.

Referencias

Angeloni, R., Contreras Ramos, R., Catelan, M., et al. 2014, A&A, in press
Bono, G., Castellani, V., & Marconi, M. 2000, ApJ, 532, L129
Casali, M., Adamson, A., Alves de Oliveira, C., et al. 2007, A&A, 467, 777

Catelan, M., Minniti, D., Lucas, P. W., et al. 2011, Carnegie Obs. Conf. Ser., 5, 145
Catelan, M., Minniti, D., Lucas, P. W., et al. 2013, in 40 Years of Variable Stars: A Celebration of Contributions by Horace A. Smith (ed. K. Kinemuchi, H. A. Smith, N. De Lee, & C. Kuehn), p. 141
Catelan, M., Pritzl, B. J., & Smith, H. A. 2004, ApJS, 154, 633
Dékány, I., Minniti, D., Catelan, M., Zoccali, M., Saito, R. K., Hempel, M., & Gonzalez, O. A. 2013, ApJ, 776, L19
Dekany, I., Minniti, D., & Saito, R. K. 2014, ATel, 5954, 1
Ferreira Lopes, C. E., Dékány, I., Catelan, M., Cross, N. J. G., Angeloni, R., Leão, I. C., & De Medeiros, J. R. 2014, A&A, submitted
Gillessen, S., Eisenhauer, F., Trippe, S., et al. 2009, ApJ, 692, 1075
Hempel, M., Minniti, D., Dékány, I, et al. 2014, The Messenger, 155, 24
Jurcsik, J., & Kovács, G. 1996, A&A, 312, 111
Kovács, G., & Walker, A. R. 2001, A&A, 371, 579
Layden, A. C. 1995, AJ, 110, 2312
Minniti, D., Lucas, P. W., Emerson, J. P., et al. 2010, NewA, 15, 433
Morgan, S. M., Wahl, J. N., & Wieckhorst, R. M. 2007, MNRAS, 374, 1421
Nemec, J. M., Cohen, J. G., Ripepi, V., Derekas, A., Moskalik, P., Sesar, B., Chadid, M., & Bruntt, H. 2013, ApJ, 773, 181
Robitaille, T. P., Meade, M. R., Babler, B. L., et al. 2008, AJ, 136, 2413
Saito, R. K., Hempel, M., Minniti, D., et al. 2012, A&A, 537, A107
Saito, R. K., Minniti, D., Angeloni, R., et al. 2013, A&A, 554, A123
Schlegel, D. J., Finkbeiner, D. P., & Davis, M. 1998, ApJ, 500, 525
Simon, N. R., & Lee, A. S. 1981, ApJ, 248, 291
Simon, N. R., & Teays, T. J. 1982, ApJ, 261, 586
Soszyński, I., Dziembowski, W. A., Udalski, A., et al. 2011, AcA, 61, 1
Stellingwerf, R. F. 1978, ApJ, 224, 953
Stetson, P. B. 1996, PASP, 108, 851
Udalski, A., Szymanski, M., Kaluzny, J., Kubiak, M., & Mateo, M. 1992, AcA, 42, 253
Welch, D. L., & Stetson, P. B. 1993, AJ, 105, 1813
Zechmeister, M., & Kürster, M. 2009, A&A, 496, 577